Two-way Analysis of Steel-deck Floor Slabs

Max L. Porter

Ninth International Specialty Conference on Cold-Formed Steel Structures
St. Louis, Missouri, U.S.A., November 8-9, 1988

Two-Way Analysis of Steel-Deck Floor Slabs

Max L. Porter*

Summary

A strength analysis procedure was formulated for five full-scale two-way test slabs reinforced with composite cold-formed steel decking. The slabs were subjected to four concentrated loads. The analysis was founded on the principles of yield-line theory and of shear-bond regression analysis. A yield-line collapse mechanism was utilized to determine the width of an effective load-carrying segment for which the total load capacity was found by totaling the reactive shears on all sides of the segment.

Introduction

An extensive theoretical and experimental research program on steel-deck-reinforced floor slabs was undertaken at Iowa State University (ISU) and under the sponsorship of the American Iron and Steel Institute (AISI). A total of 353 specimens were tested [6]. The material presented in this paper will focus on the analysis of two-way simply supported floor slabs reinforced with cold-formed steel decking. The results of tests of five full-scale two-way simply supported slabs, discussed previously [3,8], will be utilized as the basis for the analysis contained in this paper. In addition, this paper will utilize the previous information gained from the analysis involving the strength prediction and design recommendations of one-way slab elements [7]. Previous ISU research has indicated that the predominate mode of failure for composite steel-deck-reinforced slab elements is that of shear-bond. Porter et al. [9] gives information as to the development of the shear-bond prediction equations which will be incorporated into the analysis given in this paper. The comparison of test results with shear-bond design predictions is given in [5].

A common method of analysis and design for steel-deck-reinforced floor slabs is to consider the system as a one-way floor slab. However, questions arise as to the amount of distribution of forces in the so-called "weak" direction transverse to the deck corrugations, particularly for floor slabs subjected to concentrated loading. Behavioral characteristics from tests of the full-size floor slabs with applied concentrated loads (such as those from a fork-lift truck)

*Professor, Department of Civil Engineering, Iowa State University, Ames, Iowa 50011.

are given by Porter and Ekberg [2,8]. These test results provide a basis for the two-way method of analysis described in this paper. The overall intent of this investigation was to provide information which would be helpful for the design of steel-deck slab systems subjected to concentrated loads. This paper will focus on a proposed analysis procedure to predict the failure mechanism for concentrated loads on steel-deck-reinforced slabs as similarily comprised in the mechanism analysis procedures for ordinary reinforced concrete slabs discussed in Braestrup's paper on "Punching Shear in Concrete Slabs" [1].

Description of Full-Scale Slab Tests

All five test slabs analyzed in this paper were simply supported as shown in Fig. 1. The first slab tested contained corner restraints, whereas the corners of the remaining slabs were free to lift upward. All slabs had nominal out-to-out plan dimensions of 16 ft. by 12 ft. (4.88 m by 3.66 m) with the steel deck corrugations paralleling the 12 ft. (3.66 m) sides. Four slabs had a nominal thickness of 4 5/8 in. (11.8 cm) and one a thickness of 5 1/2 in (14 cm). The five test slabs were composed of steel deck sections obtained from three different manufacturers. Table 1 in [8] provides a data summary of the significant material properties for each slab including supplementary reinforcing. Additional details concerning the slab tests are available in [2] and [4]. Loading of all five slabs consisted of four concentrated loads located as shown in Fig. 1. Details of the loading apparatus and procedure are available in [2] and [8].

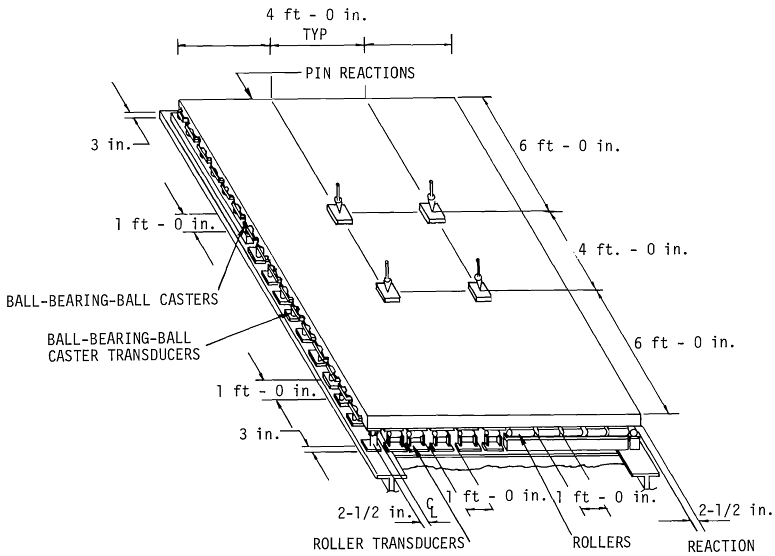

Fig. 1. General configuration and support conditions for full-scale slab tests.

Table 1 contains a summary of the applied ultimate and cycling loads for each of the five slabs. These loads are tabulated on the basis of the amount applied at each of the four concentrated points and include the weight of the loading apparatus, but do not include the slab dead weight.

Table 1. Experimental and predicted one-way, shear-bond loads for the five full-scale slab tests.

Slab No. (1)	Cycling Load--Kips per Load Point (2)	Ultimate Load--Kips per Load Point (3)	Equivalent Ultimate Uniform Load--psf (4)	Calculated One-way Shear-bond Uniform Load, W_u--psf (5)
1	None	13.7	305	256
2	9.4	15.5	345	239
3	6.4	8.8	196	243
4	9.4	14.4	320	490
5	5.4	9.4	209	247

Note: 1 kip = 4448N; 1 psf = 47.9 N/m^2

In conjunction with the ultimate loads shown in Table 1, it is important to note the type of failure that occurred. All five slabs failed ultimately by shear-bond. This failure was characterized by a horizontal end-slippage accompanied by the development of diagonal cracks over the central regions on the vertical faces at the east and west sides of the slabs. This end slippage was similar to that experienced in one-way slab element tests, except that the slippage for the two-way specimens occurred over the central regions. Details on the behavioral characteristics of the failure of the slabs are available in [2] and [8].

One-Way Shear-Bond Analysis

Present recommended design procedures [7] for steel-deck-reinforced floors utilize the concept of a one-way conventionally reinforced slab. As a means of illustrating the two-way strength, the one-way capacity was computed for each of the five slab tests. The shear-bond regression method of one-way analysis [5, 7, 9] was employed to give approximate ultimate uniform loads.

The calculated shear-bond capacity values given in Table 1 were obtained from the following equation [7,9], for a unit width of 12 in (30.48 cm):

$$V_u = \frac{12d}{s}\left(\frac{k_1 \rho d}{L'} + k_2\sqrt{f'_c}\right) \tag{1}$$

where

V_u = shear-bond capacity of a one-way slab element in pounds per foot of width

k_1 and k_2 = slope and intercept, respectively, of a shear-bond regression analysis [5, 7, 9]. These values were obtained from previous tests on slab elements with identical steel decking.

f'_c = compressive strength of concrete, in psi

d = effective slab depth as measured from extreme concrete compression fiber to centroidal axis of steel deck, in inches

s = center-to-center spacing of wires for a spot-welded shear transferring device, in inches (for cases of embossments where the shear transferring device is a fixed pattern, the value of s is unity)

L' = shear span length, in inches; L' = 45.5 in (11.56 cm) for all five slabs

ρ = reinforcement ratio, $A_s/bd = A_s/12d$ for a per foot of width computation

A_s = cross section area of steel deck where used as tension reinforcement, in^2/ft of width.

As can be seen, the correlated one-way values do not give a consistent prediction of the two-way capacity of the slabs subjected to the four concentrated loads. This inconsistency would be somewhat expected since the one-way element does not properly account for the correct width of the concentrated load distribution in the direction transverse to the steel deck corrugations.

Combined Shear-Bond and Yield-Line Analysis

The five test slabs ultimately failed via end-slip, typifying a shear-bond failure. However, at failure, the crack pattern developed was identical to that expected from a yield-line collapse mechanism. In fact, the effective width measured from the crack patterns matched that established by the controlling yield-line mechanism [2]. This flexural behavior is compatible with the shear-bond failure mode due to the combined action of shear-bond and flexure at failure. Thus, a method of analysis which combines the shear-bond and the yield-line theory approaches seems logical as a means of predicting the ultimate strength of the two-way steel-deck-reinforced floor slabs subjected to concentrated loads.

The concept involves first establishing the proper yield-line mechanism which provides the effective load-carrying width and then applying the principles of the shear-bond approach to the effective load-carrying segment established by the mechanism. Fig. 2 shows the collapse mechanism and the effective load-carrying segment used for analysis of the five two-way slab tests.

Ordinarily, the mechanism in Fig. 2 would be used to predict a flexural type of slab failure. However, for this combined analysis the yield-line theory was used only to establish the collapse mechanism. Even though the five test slabs failed ultimately by shear-bond, the observed crack patterns (presented in [2] and [8]) conformed with the yield-line collapse mechanism. Therefore, the yield-line theory was used to define the crack pattern for the collapse mechanism and subsequently establish the effective load-carrying segment of width L" in Fig. 2.

Determination of the effective width, L", of the load-carrying segment permitted computation of the vertical shear forces resisting the downward applied loads for the load-carrying segment. The two shear forces computed were V_T and V_L, shown in Fig. 2. The V_L shear force was computed using the shear-bond regression analysis applied to a one-way slab element parallel to the deck corrugations as shown by section A-A in Fig. 2. This longitudinal shear, V_L, was computed using a modified version of the shear-bond Eq. (1) to account for the average shear span over the shear-bond failure region of the L" width. The trapezoidal section over which shear-bond failure was assumed to occur is designated in Fig. 2 by the region marked ABCD. The results of the computations and some of the other pertinent items for the application of the shear-bond analysis in conjunction with the yield-line collapse mechanisms are presented in Table 2. The L" length values in the table were obtained from a yield-line analysis of the collapse mechanism shown in Fig. 2 and were verified by the experimental tests.

The V_T shear force was obtained from a one-way slab element transverse to the steel deck corrugations, as shown by Section B-B in Fig. 2. This transverse shear force, V_T, was obtained by two different criteria and the lower value of the two was taken as the controlling V_T force. One V_T criterion was based on the shear strength of the concrete above the neutral axis, assuming a cracked section as not contributing shear below the neutral axis.

Table 2. Computed values for the application of the shear-bond analysis in conjunction with the yield-line collapse mechanism.

Slab No.	L", See Fig. 4 (ft)	Average Overall Slab Depth (in.) (1)	Avg. Depth of Load-carrying Slab Element (in.) (2)	μm for Load-carrying Slab Element (ft-k/ft) (3)	$V_T = \frac{12\beta L d_n f'_c}{1000}$ (kips/L.P.) (4)	$V_T = \frac{\beta L \mu m}{L'' - 4}$ (kips/L.P.) (5)	V_L Eq. 8 (kips/L.P.) (6)	CALC P_u $V_T + V_L$ (kips/L.P.) (7)	EXP P_{ue} (kips/L.P.) (8)	Ratio of CALC/EXP (9)
1	8.4	4.83	5.04	1.24	4.12	3.26	9.26	12.52	13.7	0.91
2	10.1	4.62	4.75	2.86	5.65	5.42	10.75	16.17	15.5	1.04
3	8.3	4.63	4.73	0.86	0.00	2.30	8.45	8.45	8.8	0.96
4	9.4	4.68	4.90	2.56	7.01	5.49 3.88*	16.62 (11.75)*	22.11 (15.63)*	14.4	1.54 (1.08)*
5	7.4	5.44	5.46	0.56	1.90	1.90	6.91	8.81	9.4	0.94

*Based on an elliptical interaction of V_T and V_L on T-wire spot weld strength.

Note: 1 kip = 4448 N; 1 ft = 0.305 m; 1 in = 2.54 cm; 1 ft - kip/ft = 4448 m - N/m.

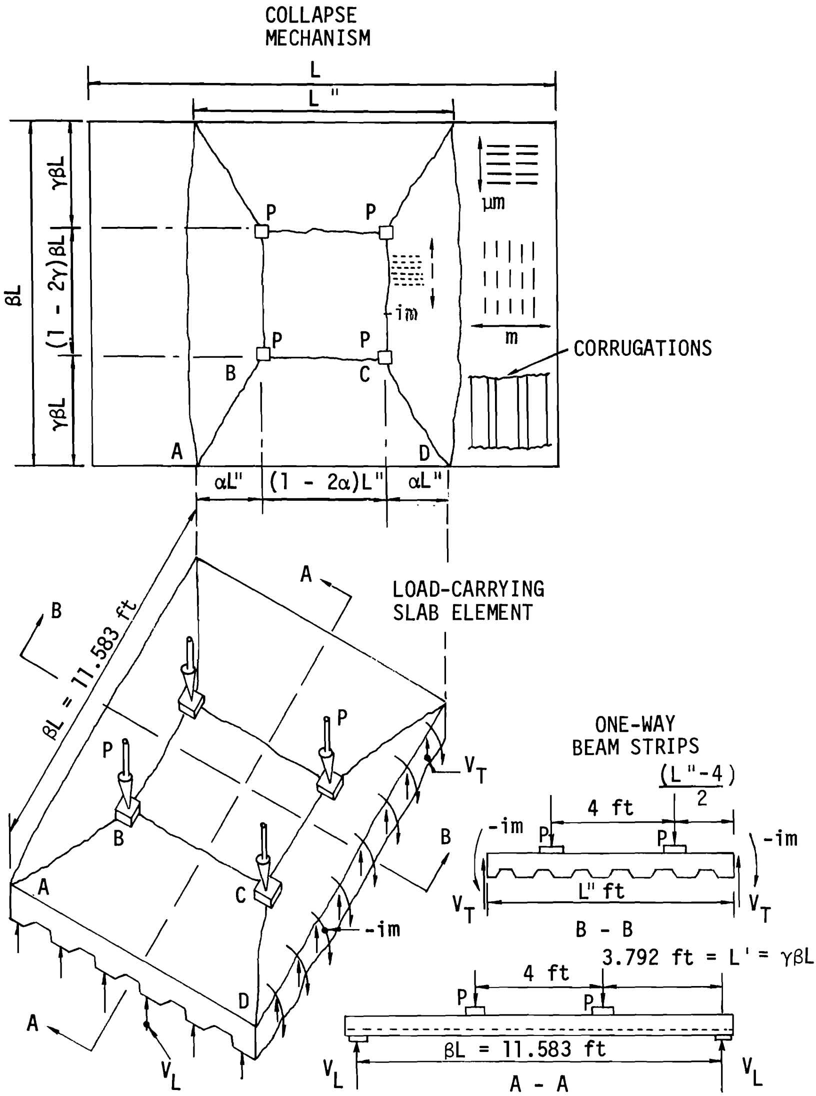

Fig. 2. Collapse mechanism and effective load-carrying segment used for analysis of five full-scale slabs.

The second V_T shear force was the smaller of the concrete shear strength or the statical shear at maximum transverse flexural capacity. Additional shear contributions from aggregate interlocking and shear friction in a cracked section are neglected.

The two criteria for computing the transverse element shear, V_T, are given by columns 4 and 5 in Table 2. The V_T force in column 4 was based on assuming a concrete shear strength of $2\sqrt{f'_c}$ for a depth above the neutral axis, neglecting any shear contribution below the neutral axis. A value of zero for the depth to the neutral axis was conservatively assigned to Slab 3, since no transverse supplemental reinforcement existed for this slab. The other criterion for V_T as given in column 5 of Table 2 was based on the shear developed in a beam strip upon reaching its flexural capacity. Section B-B of Fig. 2 illustrates a transverse beam segment with a resulting shear span (L" - 4) where L" is in feet and the four represents the distance between load points. Taking V_T times the shear span and equating this to the transverse moment capacity, μm, results in the indicated expression in Table 2 per foot of width for V_T.

The computation of V_L in column 6 of Table 2 is based on the one-way shear-bond strength of a beam segment parallel to the deck corrugations. This beam segment is shown by section A-A in Fig. 2. The shear-bond failure for the five slab tests was assumed to occur over the trapezoidal region marked ABCD in Fig. 2. This was verified by the experimental results, since end slip occurred over the region of L". Eq. (1) for shear-bond was modified to account for an L' shear span over a beam width of 4 ft (distance between load points) and to account for a L'/2 shear span in the triangular regions bordering AB and CD in Fig. 2.

Taking the shear-bond expression, Eq. (1), for each of the two triangular regions (see Fig. 2) with a shear span of L'/2, and for the rectangular region with a shear span of L', and rearranging terms and combining for the three regions, results in the following equation which was used in computing column 6:

$$V_L = \frac{dL''}{2000s}\left[\frac{k_1 \rho d}{L'}(1 + 2\alpha) + k_2\sqrt{f'_c}\right] \tag{2}$$

where the notation is the same as for Eq. (1) except that L" is the effective width in inches and α is a non-dimensional length parameter as shown in Fig. 2. The regression constants used in Eq. (5) were obtained from one-way slab element tests [5, 9]. The term "s" in Eq. (5) was unity for all slabs except Slab 4, where s was 3, since the transverse wires in Slab 4 were spaced on 3 in centers.

Once the V_T and V_L shear forces were determined, the predicted ultimate live load at each load point was found by adding the lower of the two V_T forces to the V_L force. This predicted load is shown in column 7 of Table 2. The actual experimental ultimate load per load point is shown in column 8 followed in column 9 by the ratio of calculated to experimental, representing the degree of closeness for the computed to actual ratios of values.

As can be seen by column 9, the computed values compare quite closely to the experimental ones, except for Slab 4 which is discussed below. The ratio values of 0.91, 1.04, 0.96, and 0.94 for Slabs 1, 2, 3, and 5 are considered very good and well within normal reinforced concrete experimental variation.

The ratio of 1.54 for Slab 4 in column 9 is considered incorrect. This is due to the shear forces V_T and V_L both acting on the spot welds connecting the transverse-wires to the steel decking. The values in columns 5, 6, 7, and 9 (denoted by an asterisk for Slab 4) represent approximate reduced values to account for the interaction of V_T and V_L on the spot welds. The reduction of V_T and V_L values was accomplished by reducing the resultant as given by the expression $\sqrt{(V_T)^2 + (V_L)^2}$ [6]

The reduction was based on the use of an elliptical curve to represent the interaction strength of V_L and V_T on the spot weld strength. As can be seen in column 9 in Table 2, this method predicted the true ultimate load with an error of only 8%.

Conclusions

An ultimate strength procedure for two-way concrete slabs reinforced with cold-formed steel decking was formulated. The procedure was founded on the principles of yield-line theory and of shear-bond regression analysis. A collapse mechanism established by yield-line procedures was utilized to establish the effective load-carrying-segment width of the slabs. After the width of this segment was established, a shear-bond regression analysis was used to predict the total shear force distributed to the reactive edges perpendicular to the deck corrugations. The total shear existing along the sides of the effective load-carrying segment was subsequently added to the shear-bond components to give the predicted ultimate load for each slab. The calculated load agreed very closely with the experimental ultimate for all five slabs with only a maximum discrepancy of 9%.

Acknowledgments

The research described in this paper was supported by the Engineering Research Institute of Iowa State University through funds provided by the American Iron and Steel Institute (AISI). Valuable guidance was provided during this investigation by the AISI Task Committee on Composite Construction of the Joint Engineering Subcommittee of the Committees of Hot Rolled and Cold Rolled Sheet and Strip Producers and Galvanized Sheet Producers under chairmanship of T. J. McCabe and past chairman A. J. Oudheusden. The author wishes to extend his thanks to Dr. C. E. Ekberg for his guidance and encouragement during the course of this investigation.

Appendix -- References

1. Braestrup, M. W., "Punching Shear in Concrete Slabs," Plasticity in Reinforced Concrete, Colloquium, Copenhagen, Denmark, May 1979,

Introductory Report, International Association for Bridge and Structural Engineering, Report of the Working Commissions, Vol. 28, Zurich, Switzerland.

2. Porter, M. L., "The Behavior and Analysis of Two-Way Simply Supported Concrete Floor Slabs Constructed with Cold-Formed Steel Decking," unpublished Ph.D. dissertation, Iowa State University, Ames, Iowa, 1974.

3. Porter, M. L., "Analysis of Two-Way Acting Composite Slabs," Journal of Structural Engineering, ASCE, Paper 19424, Vol. 111, No. 1, January 1985, pp. 1-18.

4. Porter, M. L., Ekberg, C. E., Jr., "Summary of Full-Scale Laboratory Tests of Concrete Slabs Reinforced with Cold-Formed Steel Decking," Ninth Congress of the International Association for Bridges and Structural Engineering, Preliminary Report, Zurich, 1972, pp. 173-183.

5. Porter, M. L., Ekberg, C. E., Jr., "Design vs Test Results for Steel Deck Floor Slabs," Proceedings, Third International Specialty Conference on Cold-Formed Steel Structures, University of Missouri-Rolla, Rolla, Mo., 1975, pp. 792-812.

6. Porter, M. L., Ekberg, C. E., Jr., Discussion of paper "Composite Steel-Concrete Construction," by the Subcommittee on the State-of-the-Art Survey of the Task Committee on Composite Construction of the Committee on Metals of the Structural Division; Discussion paper published in Journal of the Structural Division, ASCE, March 1975, pp. 615-616.

7. Porter, M. L., Ekberg, C. E., Jr., "Design Recommendations for Steel Deck Floor Slabs," Journal of the Structural Division, ASCE, Paper 12528, Vol. 102, No. ST11, November 1976, pp. 2121-2136.

8. Porter, M. L., Ekberg, C. E., Jr., "Behavior of Steel-Deck Reinforced Slabs," Journal of the Structural Division, ASCE, Paper 12826, Vol. 103, No. ST3, March 1977.

9. Porter, M. L., Ekberg, C. E., Jr., Greimann, L. F., and Elleby, H. A., "Shear-Bond Analysis of Steel-Deck-Reinforced Slabs," Journal of the Structural Division, ASCE, Paper 12611, Vol. 102, No. ST12, December 1976, pp. 2255-2268.

Appendix -- Notation

A_s cross section area of steel deck where used as tension reinforcement, inches squared per foot of deck width

b unit slab width, inches

d effective slab depth as measured from extreme concrete compression fiber to centroidal axis of steel deck, in inches

f'_c	compressive strength of concrete, in psi
i	dimensionless coefficient designating ratio of negative moment to the positive moment capacity, m
im	negative moment capacity, ft-lb/ft
L	length of edge of slab, ft
L'	shear span length, inches
L"	effective slab width for concentrated loads as determined by yield-line mechanism
k_1	intercept of shear-bond regression curve
k_2	slope of shear-bond regression curve
m	moment capacity of slab on a cross-section perpendicular to steel dick corrugations (longitudinal moment capacity), ft-lb/ft
P	concentrated load force applied at each concentrated load point, kips
P_u	ultimate concentrated applied slab load per load point, kips
P_{ue}	total ultimate experimental applied load to slab element specimen, kips
s	center-to-center spacing of shear transfer device for other than embossments, inches (for cases of embossments, the value of s is unity)
V_L	ultimate calculated shear force for the longitudinal one-way segment parallel to the deck corrugations of the effective load-carrying portion of the slab collapse mechanism, kips per load point
V_T	ultimate calculated shear force based on a one-way slab element transverse to deck corrugations for the effective load-carrying portion of the slab collapse mechanism, kips per load point
V_u	total ultimate shear including dead load of a slab element, pounds
W_u	uniform ultimate load as found from shear-bond analysis, psf
α	dimensionless length parameter of slab designating location of concentrated loads along length of slab
β	dimensionless width parameter of slab designating ratio of width of slab to its length
βL	width of slab, ft

γ dimensionless width parameter of slab designating location of of concentrated loads along width of slab

μ coefficient of orthotropy designating ratio of transverse moment capacity to longitudinal moment capacity

μm moment capacity of slab on a cross-section parallel to steel deck corrugations (transverse moment capacity), ft-lbs/ft

ρ reinforcement ratio, A_s/bd